Analyzing Photovoltaic System Performance through Two Phase Interleaved Boost Converter and Particle Swarm Optimization-Based Maximum Power Point Tracking

Furkan Dursun[1], Ersan Kabalcı[2]
[1] Graduate School of Science and Engineering, Nevsehir Haci Bektas Veli University, Nevsehir, TURKEY
[2] Electrical and Electronics Engineering Department, Nevsehir Haci Bektas Veli University, Nevsehir, TURKEY

Corresponding author: Furkan Dursun (e-mail: iamfurkandursun@gmail.com).

Submitted on 13.06.2024, Revised on 03.07.2024, Accepted on 03.07.2024, Published online on 23.07.2024

ABSTRACT Photovoltaic (PV) systems, which convert solar energy into electricity through irradiation, play a crucial role in renewable energy generation. To ensure these systems operate efficiently and maximize power output, Maximum Power Point Tracking (MPPT) is essential. Numerous algorithms have been developed to optimize MPPT, one of which is the metaheuristic Particle Swarm Optimization (PSO) inspired by swarm intelligence. Boost converters are used to increase and regulate the voltage and current output of PV panels, ensuring they operate at the MPP under varying irradiation and temperature conditions. The synergy between boost converters and PSO-based MPPT has been examined, revealing significant potential in enhancing energy harvesting efficiency. Simulations and experimental validations demonstrate that the proposed integration outperforms traditional MPPT techniques. This article presents a comprehensive study on the implementation of a boost converter and the use of the PSO algorithm for MPPT in PV systems. The research contributes to the sustainable use of solar energy resources by enhancing the reliability and efficiency of PV systems. The findings offer substantial insights into the intricate design and optimization processes of photovoltaic installations. These insights are pivotal in advancing the efficiency and reliability of PV systems, which in turn, facilitate the broader adoption of renewable energy technologies. By addressing critical aspects of PV system performance and improving energy harvesting capabilities, this research accelerates the adoption of renewable energy, supports global sustainability efforts, and promotes a cleaner, greener energy landscape.

KEYWORDS Boost converter, Particle Swarm Optimization, Photovoltaic Panels, Renewable Energy, Sustainability.

1. INTRODUCTION

The energy demand increasing rapidly all over the world. Conventional methods which are coal, crude oil, and natural gas generate varying emission gases such as carbon dioxide, methane, etc. during the burning section. And these are cause climate change and air pollution. Moreover, these fossil fuels cannot be found constantly in nature. Consequently, these issues are led people to use renewable energy sources [1].

In research of sustainable and renewable energy sources, photovoltaic (PV) systems have emerged as a hopeful technology for harnessing solar energy. PV panels that are made of semiconductor metals convert sunlight to electrical energy, making them a renewable environmentally friendly solution for meeting energy demands. Nevertheless, the efficiency of the PV systems is based on their ability to operate at Maximum Power Point (MPP) during different environmental conditions such as partial shading, irradiation, temperature, etc. [2].

To improve the performance of PV systems, a lot of feed forward control algorithm have been developed to dynamically track the MPP. They are called Maximum Power Point Tracker (MPPT) algorithm. One of them is Particle Swarm Optimization (PSO) algorithm. It has gained magnificent attention by reason of its perform to track MPP in complex and dynamic operating conditions [3].

This article focuses on the implementation of boost converter and integration of the PSO algorithm for MPPT in PV systems with different irradiation value. This article structured as follows: Section II system description, Section III delves into PV panels, Section IV provides an insight of boost converter, two phase interleaved boost converter (TPIBC) and them using in

PV panels, definition and application of PSO algorithm given in Section V, and Section VI consists of simulation results. Lastly, Section VII provides the conclusion.

2. SYSTEM DESCRIPTION

The proposed system, which is shown in Fig.1, consist of PV panel, conventional boost converter and MPPT controller.

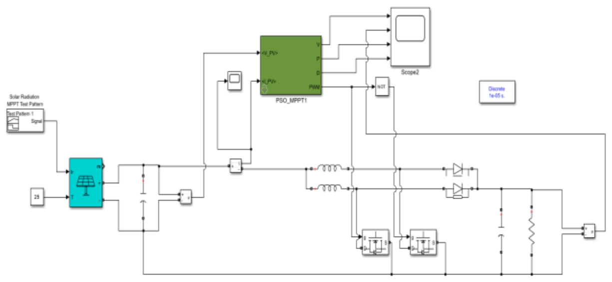

Figure 1. The Proposed System Design in MATLAB

In this system, basically, irradiation that values vary over time is applied to PV module. PSO algorithm detects change and updates the duty cycle value of the TPIBC to provide maximum power point at any time. The TPIBC acts as the link between the PV module and the load, enabling efficient power conversion and management. This converter functions by alternating between two converter phases, thereby diminishing both input and output current ripple, which boosts system stability and enhances overall efficiency. The PV module acts as the main renewable energy source within the system, transforming sunlight into electrical energy that is subsequently directed to the TPIBC for additional processing. The efficiency of the system heavily relies on the performance attributes of the PV module, such as irradiance level and temperature, which play pivotal roles. The PSO algorithm enhances TPIBC operation by dynamically tweaking its duty cycle value, aiming for peak efficiency in power transfer.
When combined, the TPIBC, PV module, and PSO algorithm create a closed-loop control system that dynamically enhances both power transfer efficiency and performance. The PV module collects solar energy, which is subsequently processed by the TPIBC to fulfill the load demands. In the meantime, the PSO algorithm consistently fine-tunes the TPIBC's control parameters to guarantee optimal performance amidst fluctuations in conditions like irradiance levels and load requirements. Overall, the integration of the TPIBC, PV module, and PSO algorithm presents a holistic solution for enhancing the efficiency and effectiveness of solar energy harvesting systems. This integration ensures heightened adaptability and responsiveness to environmental fluctuations and load variations, thereby optimizing overall system performance.

3. PV PANELS

PV Panels generates electricity from solar radiation. The physical structure of a PV system is consisting of a metal grid on the top, a metal base on the bottom and a semiconductor layer between of them. Material of semiconductor layers may change in the manufacturing process. Most solar systems are produced crystalline silicon (c-Si) solar cells made of polycrystalline or monocrystalline [4].

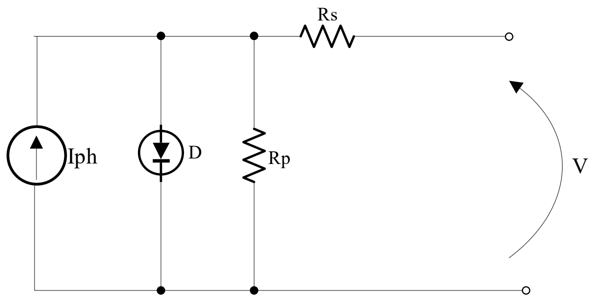

Figure 2. Basic Diagram of Photovoltaic Cell

The equivalent circuit photovoltaic cell is shown in Figure 2, that consist of a current source, diode, and resistors. In practice, the actual I-V characteristic of a solar cell typically deviates to some degree from the ideal characteristic. A common approach involves utilizing a two-diode model to accurately represent the observed curve, where the second diode incorporates an 'ideality factor' of 2 within the exponential term's denominator. In addition, the solar cell (or circuit) may feature series resistance (R_s) and parallel resistance (R_p), contributing to a characteristic format where the light-generated current I_{ph} might, under certain conditions, vary with voltage. The equation of I-V characteristic for ideal PV given Eq. (1) [5]:

$$I = I_{ph} - I_{o1}\left\{\exp\left(\frac{V+IR_s}{k_B T}\right)-1\right\} - I_{o2}\left\{\exp\left(\frac{V+IR_s}{2k_B T}\right)-1\right\} - \frac{V+IR_s}{R_p} \quad (1)$$

This study used two series-connected Panasonic N250 panels that have Heterojunction with intrinsic Thin-layer (HIT) technology. PV specifications which is used in the proposed system shown in Table 1.

The proposed system subjects the PV panel to a constant temperature of 25°C and varying levels of irradiation during different time periods. To provide this information, graphs of irradiation value and time, as well as power output, are displayed in Figure 3 and Figure 4, respectively.

Table 1
PV Specifications

Maximum Power	P_{MAX} = 250W
Voltage at MPP	V_{MPP} = 44.3 V
Current at MPP	I_{MPP} = 5.56 A
Open Circuit Voltage	V_{OC} = 53.2 V
Short Circuit Current	I_{SC} = 6.03 A
Temperature Coefficient of I_{sc}	α = 0.102 A/ ºC

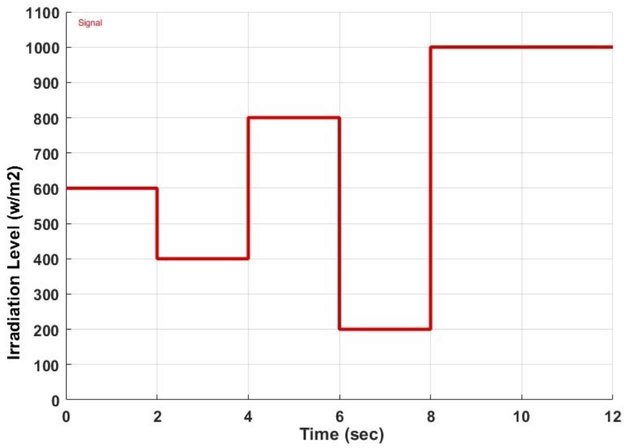

Figure 3. Solar Irradiation Values of PV Panel

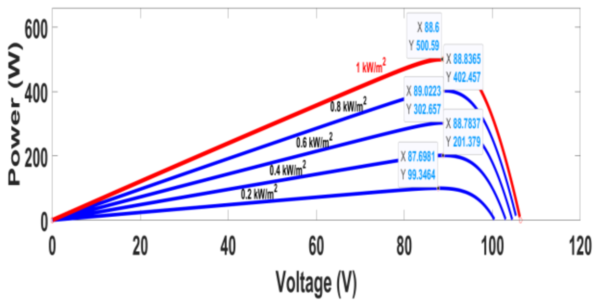

Figure 4. Characteristics of the PV cell

Based on the graphs, it can be observed that the PV module generates a maximum power of 500W at an irradiation of 1000 W/m^2. At an irradiation of 800 W/m^2, the module generates a maximum power of 400 W. Similarly, at 600 W/m^2 and 400 W/m^2 irradiation, the module generates a maximum power of 300W and 200W respectively. Finally at 200 W/m^2 the module generates 100W output power.

In this proposed system, the PV panel has specific time intervals where it can produce its maximum power. During the first 0-2 seconds, the maximum power output is 300W. Second 2-4 seconds, the maximum power output is 200W.From 4-6 seconds, the maximum power output increases to 400W. The highest power output of 100W is achieved during 6-8 seconds, and the maximum power output in the 8-12 second interval is 500W at most.

4. BOOST CONVERTERS

4.1. Conventional Boost Converter

Within the literature, different voltage-converting methods have been documented, incorporating essential energy storage components such as inductors and capacitors, as well as transformers, in combination with switches and diodes within the circuit [6]. Power converters have become more widespread with the development of semiconductor switching elements such as MOSFET (Metal Oxide Semiconductor Fiel Effect Transistor) and IGBT (Insulated Gate Bipolar Transistor), One of those converters is the boost converter. The boost converter is capable of increasing the output power beyond the input power [7]. Voltage-boosting DC-to-DC converters find widespread use in diverse power conversion applications, ranging from sub-voltages to tens of thousands of volts, and handling power levels spanning from milliwatts to megawatts. Boost converter's circuit is shown in figure 5.

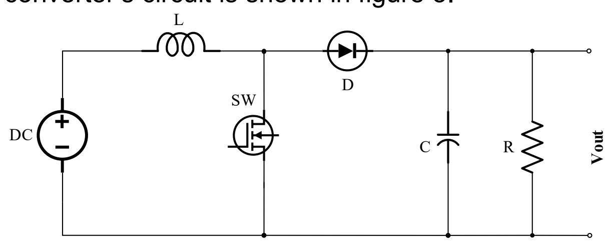

Figure 5. Circuit of Boost Converter

In this circuit, the duty cycle is calculated with Eq. (2) and Eq. (3) where D is duty cycle, Vin is input voltage and V_{out} is output voltage;

$$Vo = \frac{Vin}{1-D} \tag{2}$$

$$D = 1 - \frac{Vin}{Vout} \tag{3}$$

The voltage equation of the step-up converter circuit shows that the output voltage value is directly related to the duty cycle. When the duty cycle is high, the output voltage increases. Most boost converter designed for continuous-current operation. Continuous conduction mode (CCM) is a state of the converter where the inductor current remains non-zero throughout its operational period.

To operate at CCM and limit the output voltage ripple, the boundary values of inductor and capacitor are necessary in the circuit. Values are given Eq. (4) and Eq. (5);

$$L_b = \frac{(1-D)^2 DR}{2f} \quad (4)$$

$$C_{min} = \frac{DVo}{VrRf} \quad (5)$$

D is duty cycle, R is resistor value, Vo is output voltage, Vr is ripple voltage of output, and *f* is switching frequency [8].

4.2. Two Phase Interleaved Boost Converters (TPIBC)

In the realm of solar energy, the conventional boost converters that have served as stalwarts in various applications fall short when applied to photovoltaic (PV) systems. These converters, designed to increase voltage from a DC source, struggle to adapt to the variable output of solar panels.

The Two-phase interleaved converters offer more advantages than traditional boost converters in the PV panel field. An interleaved boost converter is used to decrease the input and output voltage ripples, which in turn reduces the size of filters. By dividing the output current into N parts, it reduces the I2R and inductor losses, resulting in higher efficiency. As a result, two-phase interleaved converters exhibit higher efficiency when compared to conventional boost topologies. The proposed TPIBC has shown in figure 6 [9].

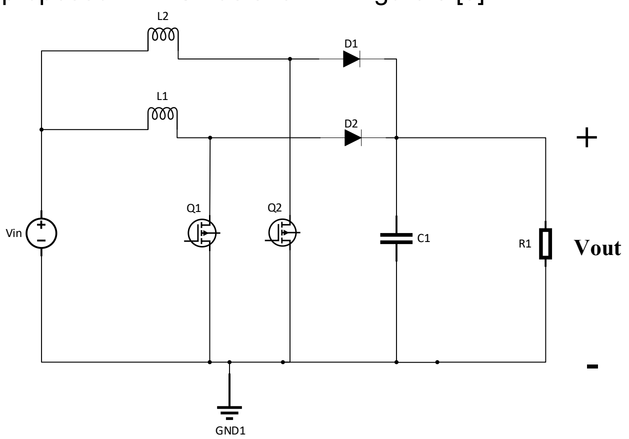

Figure 6. Proposed TPIBC

V_{in} – Input Voltage
V_{out} – Output Voltage
L_1, L_2 – Inductors
C_1 – Capacitor
R_1 – Load Resistor
T_s – Switching Period
$F_s = \frac{1}{T_s}$ – Switching Frequency
VL_1 – Voltage of L1
VL_2 – Voltage of L2
Δ_{iL1} – Current Ripple of L1
Δ_{iL2} – Current Ripple of L2
D – Duty Cycle

The TPIBC can be examined with two operation modes that are described below.

4.2.1) Mode – 1 Operation

In this mode, Q1 switch is off, Q2 switch is on, the circuit diagram has given below.

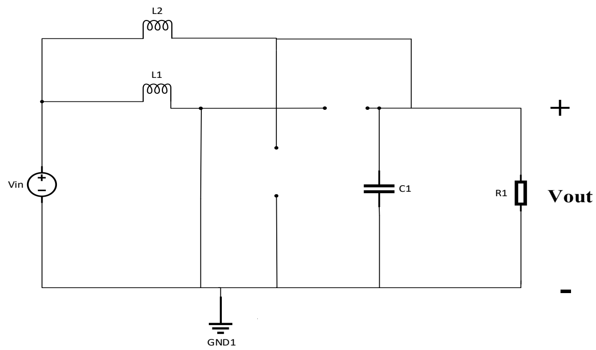

Figure 7. Mode - 1 Circuit Diagram

The voltage of L1 inductor can calculated with Eq. (6) and Eq. (7):

$$V_{L1} = V_{in} = (L_1) * \left(\frac{di_{L1}}{dt}\right) = (L_1) * \left(\frac{\Delta i_{L1}}{DT_s}\right) \quad (6)$$

$$(\Delta i_{L1})_{S1-closed} = \left(\frac{V_{in}}{L_1}\right) * DT_s \quad (7)$$

As a result of above equations, we see that the voltage of L_1 is increasing linearly. Similarly, the voltage of L_2 inductor obtained with Eq. (8) and Eq. (9):

$$V_{L2} = V_{in} - V_0 = (L_2) * \left(\frac{di_{L2}}{dt}\right) = (L_2) * \left(\frac{\Delta i_{L2}}{DT_s}\right) \quad (8)$$

$$(\Delta i_{L2})_{S1-closed} = \left(\frac{V_{in} - V_o}{L_2}\right) * DT_s \quad (9)$$

Considering the above equations, it can be concluded that since the voltage value Vo is greater than the value Vin, the current passing through the L2 inductor decreases linearly.

4.2.2) Mode – 2 Operation

In this mode, unlike the mode 1, Q1 is on, Q2 is off, the circuit diagram shown in Figure 8.

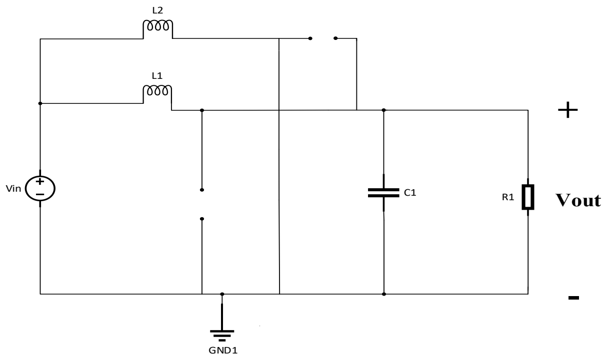

Figure 8. Mode - 2 Circuit Diagram

This mode is opposite of the previous mode. So that, the inductor L_1 stores energy and L_2 transfers it to the load through D_2.
L_1 inductor voltage equations are;

$$V_{L1} = (V_{in} - V_o) = (L_1) * \left(\frac{di_{L1}}{dt}\right) = (L_1) * \left(\frac{\Delta i_{L1}}{(1-D) * Ts}\right) \quad (10)$$

$$(\Delta i_{L1})_{S2-closed} = \left(\frac{Vin - Vo}{L_1}\right) * (1-D)Ts \quad (11)$$

As a consequence of the above equations, because of Vo greater than V_{in} current of L_1 decreasing linearly. The voltage of L_2 inductor is [10];

$$V_{L2} = V_{in} = (L_2) * \left(\frac{di_{L2}}{dt}\right) = (L_2) * \left(\frac{\Delta i_{L2}}{(1-D) * Ts}\right) \quad (12)$$

$$(\Delta i_{L2})_{S2-closed} = \left(\frac{V_{in}}{L_2}\right) * (1-D)Ts \quad (13)$$

With these equations, the component values of proposed TPIBC are shown in Table II.

Table 2
Component Values of Two-Phase Interleaved Boost Converter

Parameter	**Value**
C_1,C_2 Capacitors	10 uF
L_1, L_2 Inductors	2 mH
fs, converter switching frequency	10 kHz
Vi, converter input voltage	88.6 V
Vo, converter output voltage	250 V

The output power of a solar cell can be affected by various factors such as irradiation and temperature, and its efficiency is typically low. Therefore, it is important to have an MPPT system that provides the maximum power to boost converter [11].

5. PARTICLE SWARM OPTIMIZATION (PSO) ALGORITHM

A MPPT is normally employed in conjunction with the power converters to optimize the utilization of large arrays of PV modules. The main reason for using MPPT in the PV arrays is to capture maximum power peak and provide stability. Nevertheless, because of changing environmental conditions such as irradiation, temperature, etc. The peak point of power fluctuates non-linearly [12].

To handle these fluctuations, various MPPT algorithms have been developed over the years. Among them, the Perturb and Observe (P&O) method is widely used. It works by perturbing the operating voltage of the solar panel in a given direction. If the power output increases, it means that the panel is moving closer to the MPP, so the algorithm continues to perturb the voltage in the same direction. If the power output decreases, it means that the panel is moving away from the MPP, so the algorithm reverses the direction of the perturbation. This method enough and good to reach the MPP is independent of the PV panel but may be affected by rapid changes in environmental conditions.

The other using widely MPPT method is incremental conductance (IC). Similar to the perturb and observe method, the incremental conductance method achieves the maximum power point in the same manner. But IC method is not affected by fast changes in irradiation, temperature or environmental conditions [13].

Besides the P&O and IC algorithms, there are many MPPT algorithms for PV panel. When we consider P&O and IC algorithms, both of them have disadvantages. For instance, P&O cannot operate MPP under instantaneous weather changing conditions. IC method is good at operating MPP with rapidly changing weather conditions but it needs costly and complex control mechanisms, so P&O and IC are not the adequate solution for partial shading conditions and they can't respond to fast transient changing [14].

To cope with these issues and to ensure that operating PV panels are under rapidly changing weather conditions and irradiations, particle swarm optimization (PSO) has been used as MPPT for PV in the literature. PSO is a metaheuristic algorithm in 1995, Eberhart and Kennedy developed this technique based on the social behavior of bird flocking and fish schooling.

PSO is swarm-based algorithm and depend on swarm intelligence. Each member of PSO called particle and the population created by members named swarm in PSO. The particle has its own speed and position to attain the optimal result for algorithm. The movement of particle shown in figure 9;

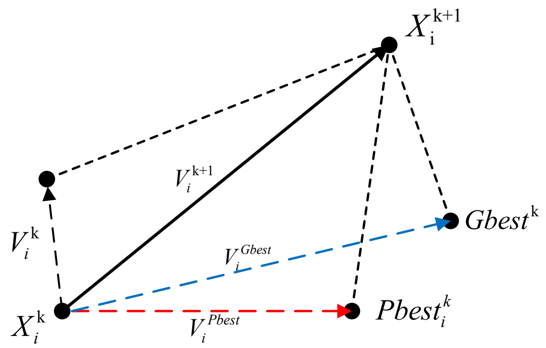

Figure 9. Particles Movement in PSO

- i: Particle
- k: Iteration
- X_i^k:Position of i particle in k iteration
- V_i^k Velocity of i particle in k iteration
- $Gbest^k$ The particle with best position in the swarm
- $Pbest_i^k$ Personal best position of i particle
- V_i^{Pbest} Velocity of Pbest particle
- V_i^{Gbest} Velocity of Gbest Particle
- X_i^{k+1} Position of i particle in k+1 iteration
- V_i^{k+1} Velocity of i particle in k+1 iteration

In the PSO algorithm, particles are initially searched with random velocity and position values. A defined quantity of particles has movement in the search space to attain the best solution. Movement of particle is altered by tracking the best position while also exploring new solutions. To find optimal solution the particle must follow either its own best position or its neighbor's position. In every iteration of the PSO algorithm, velocity and position of the particles are updated. Velocity and position of particle can be calculated as Eq. (14) and Eq. (15) [15]:

$$V_i^{k+1} = w.V_i^k + c_1.r_1.(Pbest_i^k - x_i^k) + c_2.r_2.(Gbest^k - x_i^k) \quad (14)$$

$$x_i^{k+1} = x_i^k + V_i^{k+1} \quad (15)$$

- w Inertia weight
- c_1 Cognitive coefficient
- c_2 Social coefficeint
- r_1, r_2 Random variables within [0,1]

Considering above definitions, $c1.r1.(Pbest_i^k - x_i^k)$ represent the effect of the particle's own experience on its movement. And also, $c2.r2.(Gbest_i^k - x_i^k)$ represent the effect of swarm experience on particle movement. PSO method has two basic logics; first is particle initialization, second is function evaluation. The steps tracking and covering this phenomenon of PSO. Basic flowchart diagram of the PSO has shown in Figure 10.

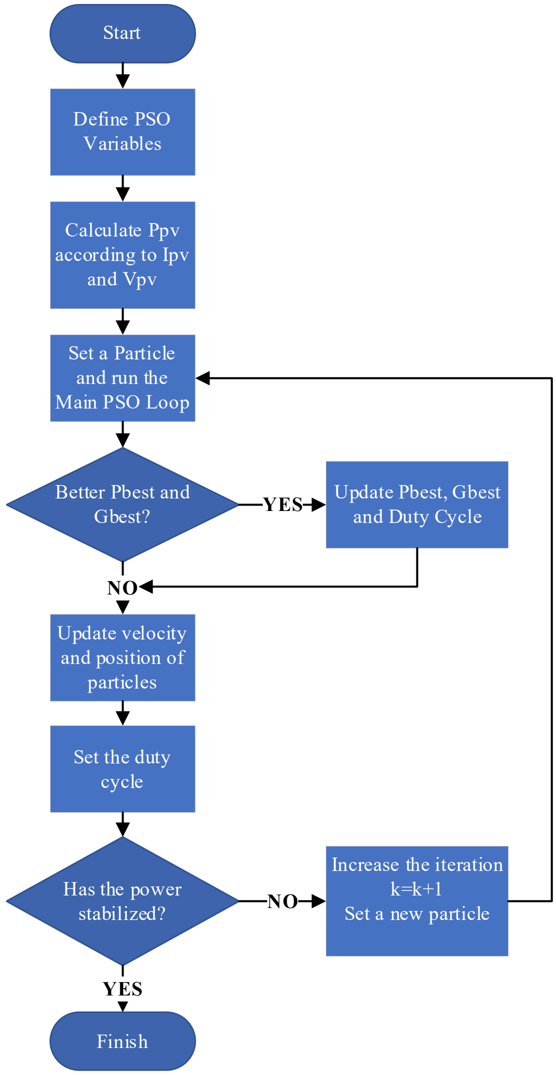

Figure 10. Proposed PSO Flowchart Diagram

In the basic PSO, there are five main steps to operate algorithm;

Step1. Define the all parameters of PSO

Step2. Calculate the value of particle

Step3. Check Pbest and Gbest value

Step4. Then update velocity and position

Step5. If the stop criterion provided, end the algorithm otherwise go to next iteration.

6. SIMULATION RESULTS

To verify the proposed MPPT algorithm, an interleaved boost circuit is designed shown in Fig. 1. The design was simulated with MATLAB.

6.1. Converter Simulations

Based on the information that was provided in the section IV, the TPIBC's input current ripple and output voltage ripple must have less than the conventional boost converter topology. In the Figure 11 and 12, the input current ripple of TPIBC is smaller than the input current ripple of conventional boost converter;

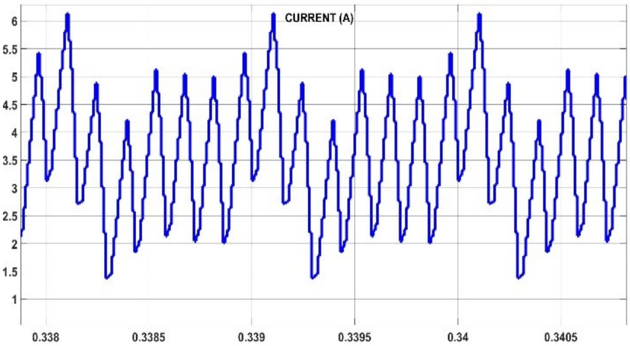

Figure 11. Conventional Boost Converter Input Current Ripple

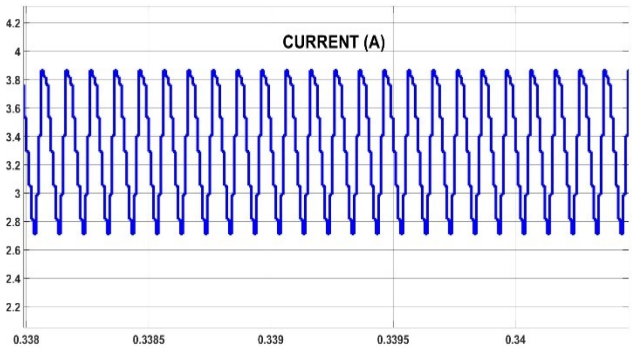

Figure 12. Two Phase Interleaved Boost Converter Input Current Ripple

These simulations provide that the conventional boost converter input current ripple started within 0-7 amperes fluctuation. On the other hand, the TPIBC input current ripple had a maximum 2.7-3.9 A fluctuation at the beginning of simulation and almost none at the end of simulation.

Besides the input current ripples, the output voltage ripples are important. Based on information in [16], output voltage ripple must be less in the TPIBC than in the classical boost converter. Figure 13 and 14 make clear that voltage differences in the TPIBC are much less than in the traditional boost converter.

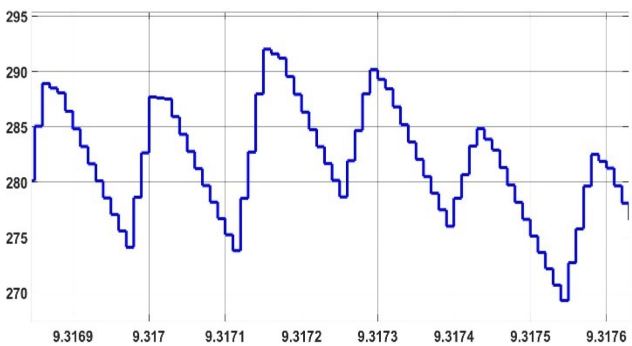

Figure 13. Conventional Boost Converter Output Voltage Ripple

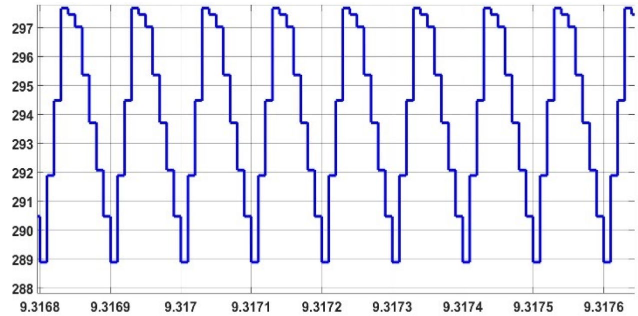

Figure 14. Two Phase Interleaved Boost Converter Voltage Output Ripple

While the voltage of traditional system fluctuates between 270-295V, this value is between 289-298V in the two-phase system. Therefore, ripple differences between these two systems are almost 20V.

6.2. Algorithm Simulations

As stated in Eq. (13) and Eq. (14) in the 5th section of the article, there are many variables in the PSO algorithm that clearly affect the algorithm results. In the simulations whose results are shown below, number of particles, cognitive coefficient, social coefficient, particle number and inertia weight, among others, are analyzed. There are many analyses but, in this section, only six main comparisons will show with figures.

6.2.1) Number of Particles

The PSO algorithm manages a group of particles, where each particle embodies a potential solution. In the context of particle swarm optimization (PSO), a "particle" symbolizes a potential solution within the optimization problem's search space. Each particle possesses both a position and a velocity within this space, which undergo iterative adjustments aimed at seeking the optimal solution [17]. The particle affect was simulated. As a result of simulations, concluded that the best result was examined when the number of particles settled as four. The two effect of particles given below in Fig. 15 and Fig. 16:

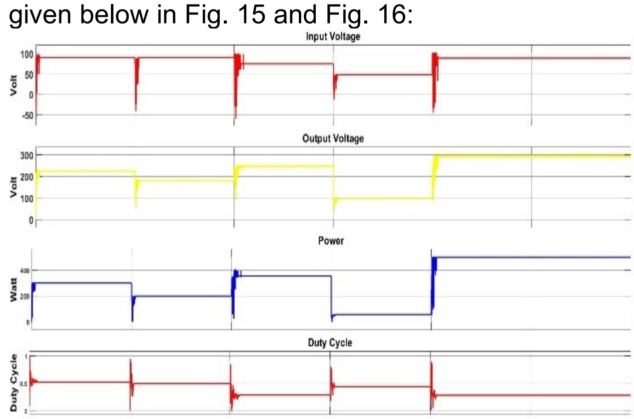

Figure 15. When the Number of Particles was Selected as 4

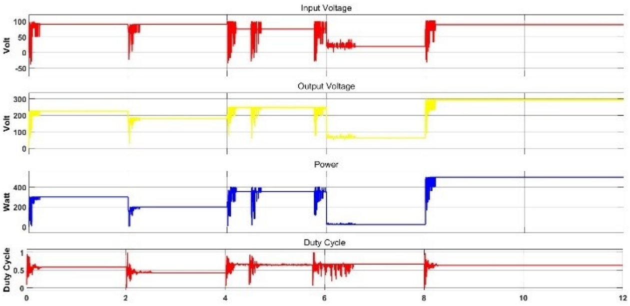

Figure 16. When the Number of Particles was Selected as 8

The first row of the graphs represents the input voltage, the second one is the output voltage, and the third and fourth are power and duty cycle of the algorithm respectively. These and all subsequent simulation graphs have the same layout.

6.2.2) Inertia Weight

The weight of inertia "w" determines how much the current velocity is influenced by the previous velocity. It ensures a balance between the exploration and exploitation stages of the optimization process. It is very important to adjust the inertia weight properly in order to achieve optimal performance in particle swarm optimization (PSO). The best solution was obtained when the inertia weight was selected as “0.5” among the 0.1 – 0.9 values. Below are the graphics of the simulation outputs when the inertia weight is selected as 0.5 and 0.9.

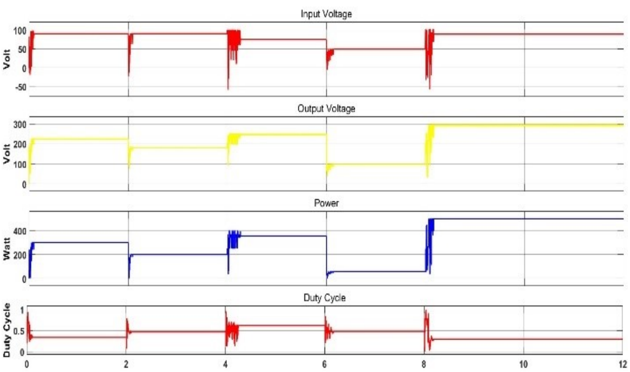

Figure 17. When the Inertia Weight was Set to 0.5

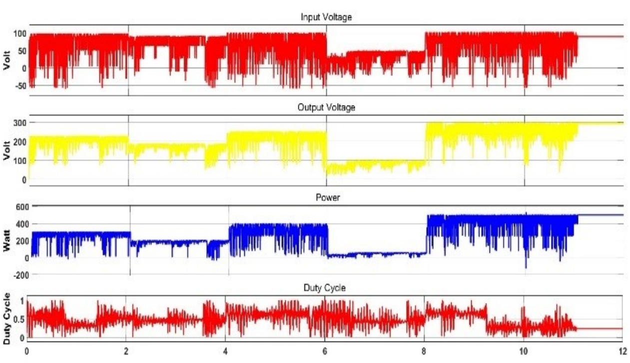

Figure 18. When the Inertia Weight was Set to 0.9

6.2.3) Cognitive & Social Coefficients

These coefficients control the particle’s tendency. While the c1 affects the tendency of the particle towards its personal best position (*pbest*), the c2 affects towards its global best position (*gbest*). If the cognitive coefficient (*c1*) and the social coefficient (*c2*) in the particle swarm optimization (*PSO*) algorithm have the same value, it indicates that both personal experience (cognitive) and collective experience (social) hold an equal weightage in operating the movement of individual particles. This can lead to a balanced exploration and exploitation strategy. In these simulations, c1 and c2 values were set equal at all times. Taking account of this information, simulations were run within 1 to 2 values same for c1 and c2. The best result was obtained when c1 and c2 values were “1”.

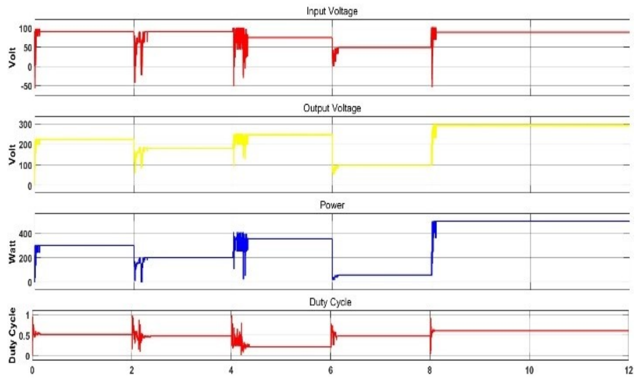

Figure 19. When the c1 & c2 Coefficient values were set "1"

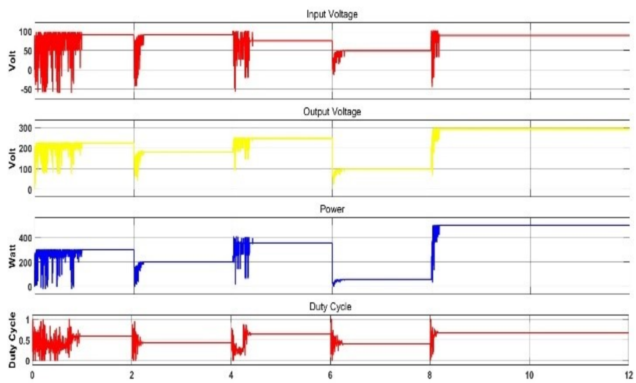

Figure 20. When the c1 & c2 Coefficient values were set "2"

Based on these simulation results, at the end of simulation, the using PSO parameters are shown the Table 3. With these PSO values, accepting 25 degrees temperature as the standard test condition (STC), the final algorithm circuit simulation in variable irradiance is shown in Figure 21. Under standard test conditions, the output power is expected to be 100W, 200W, 300W, 400W, 500W at a radiation intensity of 200 W/m^2, 400 W/m^2, 600 W/m^2, 800 W/m^2 and 1000 W/m^2 respectively.

Table 3
Parameters of The Proposed PSO Algorithm

Parameter	Value
Particle Number *n*	4
Inertia Weight *w*	0.5
Cognetive Coefficient C_1	1
Social Coefficient C_2	1

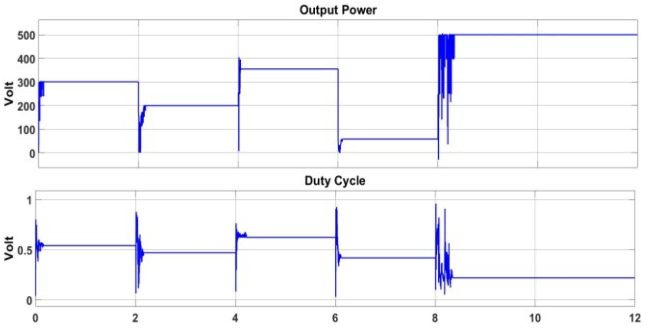

Figure 21. Main Result of Simulation

As obtained from the result in this simulation, firstly 600 W/m^2 irradiance is applied, as a result, the output power is 300W. Secondly, 400 W/m^2 irradiance is applied and the power is 200W. With the 800 W/m2 irradiation, the output power is 354W and with the 200 W/m^2 irradiation, the output power is 70W, finally, with the maximum and standard test condition level 1000 W/m^2 the output power is the expected value of 500W. The efficiency table is:

Table 4
Efficiency Table of Proposed System

200 W/m^2	400 W/m^2	600 W/m^2	800 W/m^2	1000 W/m^2
%70	%100	%100	%88.5	%100

7. CONCLUSION

This study concludes with a detailed analysis of the performance of photovoltaic (PV) systems by integrating a Two-Phase Interleaved Boost Converter (TPIBC) and Particle Swarm Optimization (PSO)-based Maximum Power Point Tracking (MPPT) algorithm. The proposed system has been extensively simulated, and it has demonstrated its ability to maximize power extraction from PV panels.

The use of TPIBC has several benefits over traditional boost converters. These include reduced output voltage ripple, improved efficiency, and enhanced reliability. Additionally, integrating PSO-based MPPT enables dynamic tracking of the maximum power point (MPP) in changing environmental conditions, maximizing the overall energy conversion efficiency of the system.

Through an investigation of the inertia weight effect, it was found that adjusting this parameter has an impact on the convergence rate and exploration-exploitation balance of the PSO algorithm. The study also examined the impact of particle number on PSO performance and found that increasing the particle number improves the global search capability of the algorithm, leading to better accuracy in locating the MPP and enhancing system robustness against environmental variations. Additionally, the analysis of the coefficients effect within the PSO algorithm clarified their influence on convergence behavior and solution quality. Fine-tuning these coefficients can significantly affect the convergence speed and exploration capabilities of PSO, which in turn affects the overall performance of the MPPT system.

Simulation results have validated the superiority of the proposed approach over conventional methods, showcasing robustness in handling rapid environmental changes. This research makes a valuable contribution to the improvement of PV system design and control, providing a practical solution for enhancing energy harvesting efficiency. In the future, efforts may be directed towards further optimization of PSO parameters, exploration of alternative converter topologies, and investigation of integration strategies with energy storage systems to maximize renewable energy utilization and grid integration.

REFERENCES

[1] E. Kabalci and A. Boyar, "Comparison of a Two-Phase Interleaved Boost Converter and Flyback Converter," in *18th International Power Electronics and Motion Control Conference*, Budapest, Hungary, 26 - 30 August, 2018, pp. 352-356.

[2] A. J. Alrubaie, A. Al-Khaykan, R. Q. Malik, S. H. Talib, M. I. Mousa, and A. M. Kadhim, "Review on MPPT Techniques in Solar System," presented at the 2022 *8th International Engineering Conference on Sustainable Technology and Development (IEC)*, Erbil, Iraq, 23-24 February 2022.

[3] R. B. A. Koad, A. F. Zobaa, and A. El-Shahat, "A Novel MPPT Algorithm Based on Particle Swarm Optimization for Photovoltaic Systems," *IEEE Transactions on Sustainable Energy,* vol. 8, no. 2, pp. 468 - 476, 2017.

[4] M. N. H. Khan, M. Forouzesh, Y. P. Siwakoti, L. Li, T. Kerekes, and F. Blaabjerg, "Transformerless Inverter Topologies for Single-Phase Photovoltaic Systems: A Comparative Review," *IEEE Journal of Emerging and Selected Topics in Power Electronics,* vol. 8, no. 1, 2020.

[5] A. Mcevoy, T. Markvart, and L. Castañer, *Pratical Handbook of Photovoltaics Fundamentals and Applications*, 2nd ed. 2011.

[6] M. Forouzesh, Y. P. Siwakoti, S. A. Gorji, F. Blaabjerg, and B. Lehman, "Step-Up DC–DC Converters: A Comprehensive Review of Voltage-Boosting Techniques, Topologies, and Applications," *IEEE Transactions on Power Electronics,* vol. 32, no. 12, 2017.

[7] M. Kumar, G. Panda, and D. V. S. K. R. K, "Analysis of Conventional and Interleaved Boost Converter with Solar

Photovoltaic System," in 2022 International Conference on Intelligent Controller and Computing for Smart Power (ICICCSP), Hyderabad, India, 21-23 July 2022.
[8] M. H. Rashid, *Power Electronics Handbook*, 3rd ed. 2011.
[9] E. Kabalci and A. Boyar, "Design and Analysis of a Two-Phase Interleaved Boost Converter Based Microinverter," in *18th International Power Electronics and Motion Control Conference*, Budapest, Hungary, 26-30 Aug. 2018, pp. 1067 - 1072.
[10] E. Kabalci and A. Boyar, "Design and Analysis of Two-phase Interleaved Boost Converter and H5 Inverter Based Microinverter," in *Global Power, Energy and Communication Conference*, 2019.
[11] G. Spiazzi, "Analysis and design of the soft-switched clamped-resonant interleaved boost converter," *CPSS Transactions on Power Electronics and Applications,* vol. 4, no. 4, 2019.
[12] A. Taylor and S. M. Musa, "Evaluation of Hybrid AI-based Techniques for MPPT Optimization," in *International Conference on Green Energy, Computing and Sustainable Technology (GECOST)*, Virtual Conference, 26-28 Oct. 2022.
[13] A. Ali *et al.*, "Investigation of MPPT Techniques Under Uniform and Non-Uniform Solar Irradiation Condition - A Retrospection," *IEEE Access,* 2020.
[14] M. Zerouali, S. Zouirech, A. E. Ougli, B. Tidhaf, and H. Zrouri, "Improvement of Conventional MPPT Techniques P&O and INC by Integration of Fuzzy Logic," in *7th International Renewable and Sustainable Energy Conference (IRSEC)*, Agadir, Morocco, 27-30 Nov. 2019.
[15] E. Kabalci and A. Boyar, "Design and Comparison of MPPT Controllers with Fuzzy Logic and Particle Swarm Optimization for PV Power Conversion," in *2nd International Conference on Control Systems, Mathematical Modeling, Automation and Energy Efficiency (SUMMA)*, Lipetsk, Russia, 11-13 Nov. 2020.
[16] S. Nahar and M. B. Uddin, "Analysis the performance of interleaved boost converter," in *4th International Conference on Electrical Engineering and Information & Communication Technology (iCEEiCT)*, Dhaka, Bangladesh, 13-15 Sept. 2018.
[17] M. N. S. Khairi, N. A. B. Bakhari, A. A. A. Samat, N. Kamarudin, M. H. M. Hussin, and A. I. Tajudin, "MPPT Design Using PSO Technique for Photovoltaic System," in *3rd International Conference in Power Engineering Applications (ICPEA)*, Putrajaya, Malaysia, 6-7 March 2023.